Available online at www.sciencedirect.com
SCIENCE DIRECT
Journal of Catalysis 242 (2006) 153–161
JOURNAL OF CATALYSIS
www.elsevier.com/locate/jcat

Changing the Si distribution in SAPO-11 by synthesis with surfactants improves the hydroisomerization/dewaxing properties

T. Blasco [a], A. Chica [a], A. Corma [a,*], W.J. Murphy [b], J. Agúndez-Rodríguez [c], J. Pérez-Pariente [c]

[a] *Instituto de Tecnología Química, UPV-CSIC, Avda. de los Naranjos s/n, 46022 Valencia, Spain*
[b] *EXXON Research and Engineering Company, 180 Park Avenue, P.O. 390, Florham Park, NJ 07932-03090, USA*
[c] *Instituto de Catálisis y Petroleoquímica, CSIC, c/Marie Curie, 2, Campus de Cantoblanco, 28049 Madrid, Spain*

Received 31 January 2006; revised 18 April 2006; accepted 20 May 2006

Available online 7 July 2006

Abstract

The silicoaluminophosphates SAPO-11 isodewaxing catalysts were synthesized with varying Si content following conventional methods and using a route involving the presence of surfactant. Smaller crystal size (∼80 nm) and higher external surface areas were found for the samples prepared with surfactant. This synthesis route using surfactant gives SAPO-11 samples with greater numbers of stronger acid sites than those prepared by conventional synthesis. The ^{29}Si MAS-NMR spectra obtained for samples containing the same amount of silicon showed that SAPO-11 prepared with surfactant contains a higher relative concentration of Si (nAl, 4-nSi), $0 < n < 4$, border environments, whereas large patches of Si(4Si) are predominant in the samples prepared without surfactant. These results support the idea that introducing surfactant during synthesis contributes to better Si dispersion, decreasing the size of Si(4Si) patches and increasing the number and strength of acid sites. The hydroconversion of n-hexadecane on Pt/SAPO-11 samples indicates that the samples synthesized with surfactant with similar Si content and very close crystallite size to those synthesized by conventional methods are much more active and selective for the hydroisomerization of long-chain n-paraffins.
© 2006 Elsevier Inc. All rights reserved.

Keywords: Silicoaluminophosphates; SAPO-11; Surfactants; Acidity; Isodewaxing

1. Introduction

The removal of long-chain n-paraffins from lubricating oils is essential to obtain a product with good cold-flow properties. Conventional lubricant dewaxing processes remove these normal paraffins by solvent extraction or by selective cracking, resulting in a yield loss directly proportional to the concentration of the normal paraffins in the oil. Catalytic dewaxing removes paraffin waxes by shape-selective hydrocracking that transform the waxes into lower-molecular weight products, which are removed from the higher-boiling lube oil by distillation. A more attractive dewaxing procedure would result from catalytic dewaxing through isomerization of the n-paraffins to branched isoparaffins, eliminating the yield loss associated with n-paraffin removal by cracking or solvent extraction [1–3]. Bifunctional molecular sieve catalysts, such as zeolite and SAPO materials, could be adequate for performing selective isomerization of the lineal alkanes through the so-called "isodewaxing" process [4,5]. In molecular sieve catalysts, selectivity could be achieved through the proper control of such variables as acidity, pore dimensions, pore topology, and crystallite size [6]. Thus, new zeolites with very different pore topologies are continuously being synthesized [7–12].

From the standpoint of hydroisomerization and hydrocracking, the acidity, pore dimensions, and topology of the zeotype catalysts have a major influence on the hydroisomerization and hydrocracking mechanisms [8–21]. Catalysts with a high degree of hydrogenation activity and a low degree of acidity are best for maximizing hydroisomerization versus hydrocracking [17]. The pore opening of the molecular sieve can also have a major effect on the selectivity of these catalysts. If the pore opening is sufficiently small to restrict the larger isoparaffins for reacting at the acid sites inside the pore, then the catalyst

* Corresponding author.
E-mail address: acorma@itq.upv.es (A. Corma).

0021-9517/$ – see front matter © 2006 Elsevier Inc. All rights reserved.
doi:10.1016/j.jcat.2006.05.027

will show good selectivity for preferentially converting normal paraffins. The ideal catalyst for selective hydroisomerization of *n*-paraffins should have both selectivity for isomerization (which comes from the accurate balance of acid and hydrogenation activity) and selectivity for preferentially reacting normal paraffins (which comes from the size and topology of the pores of the molecular sieve).

It has been shown that a bifunctional catalysts containing a noble metal (Pd or Pt) on a medium-pore unidirectional molecular sieve, such as SAPO-11 [22], ZSM-22 [23,24], or θ-1 [25], have a high isomerization/cracking ratio, with a high proportion of monobranched molecules within the isomerized products. Nevertheless, multibranched isomers seem to be predominant when the isomerization of normal alkanes with >20 carbon atoms is carried out over ZSM-22 [24]. The peculiar topology of SAPO-11 was first shown to be responsible for the high hydroisomerization selectivity seen in these materials. Restricted transition state shape selectivity has been used to explain the high selectivity for hydroisomerization [6,26–29]. According to the classical mechanism for skeletal isomerization, substituted corner-protonated cyclopropyl carbonium intermediates are formed at the molecular sieves [27–29]. It has been argued that in the branching reaction (more specifically, in the monobranching step), only part of the molecule penetrates into the micropore [28,29]. However, other authors have provided evidence that monobranching through protonated cyclopropane intermediates (CPC), followed by ring opening, also occur inside the pore [30–32]. All the foregoing works essentially put special emphasis on the topology of the molecular sieves, concluding that the unidimensional nature of the pores in SAPO-11, the crystalline size, and the moderate acidity contribute to the excellent performance for branching reactions.

Although selectivity for hydroisomerization and extension of branching is controlled by pore dimensions and topology, in principle catalyst activity should be related to the total number of active acid sites, provided that all of these sites are accessible. With respect to acid strength, it could be expected that the stronger the acidity, the lower the temperature and/or the contact time for the hydroisomerization. Then, in an optimized SAPO-11 hydrodewaxing catalyst, the number of available active acid sites also should be maximized.

It was reported that the number of acid sites in SAPO materials is related to bridging OH associated to Si–O–Al bonds, whereas their strength is a function of the proximity of acid sites, with the isolated Brønsted acid sites present in silica islands the strongest ones [33].

It is well known that the Si distribution in SAPOs, and thus the number and strength of acid sites, depend strongly on the synthesis method used. Here we show by ^{29}Si NMR, IR, and base adsorption that it is possible to modify the number and density of acid sites in SAPO-11 by introducing surfactants during the synthesis [34]. We show that through this synthesis method, it is possible to produce materials with a very unique Si framework distribution, resulting in hydrodewaxing catalysts with a much higher activity than others with the same Si content but prepared by conventional methods.

2. Experimental

2.1. Synthesis of conventional SAPO-11 samples

SAPO-11 conventional samples were prepared as described previously [35]. Accordingly, Al isopropoxide was introduced into a propylene flask with a cap provided with a hole for a stirrer. A solution of H_3PO_4 was prepared with the total amount of water (Milli-Q) required for the synthesis. The H_3PO_4 solution was added to the propylene flask, located in a H_2O bath at 293 K. The mixture was stirred for 2 h using a Teflon stirrer at 350 rpm.

After 2 h, the stirring was stopped, the necessary silica was added from LUDOX AS40, and then the mixture was stirred for another 2 h. Finally, the DPA was added, and the synthesis mixture was stirred for 2 h to form the synthesis gel. The gel prepared in this way is white, and its general composition is 1.0 Al_2O_3:1.00 P_2O_5:0.9 DPA:x SiO_2:57.0 H_2O.

The gel was distributed among six 60-mL Teflon-lined autoclaves (40 g of synthesis gel in each autoclave), and the crystallization was conducted in static mixing at 468 K for 48 h. After this, the product of each autoclave was washed with 240 mL of water and centrifuged. The samples were calcined at 823 K under a continuous flow of N_2 (130 cm^3/min) for 1 h, followed by air (130 cm^3/min) for 1 h. The solid samples of SAPO-11 were dried at 313 K and are designated as SAPO-11C.

2.2. Synthesis of SAPO-11 samples using surfactant

2.2.1. Composition range

SAPO-11 was obtained from aqueous synthesis mixtures containing phosphorous and aluminum sources, a suitable template for AEL structure (e.g., dipropylamine), a long-chain alcohol with a low solubility in water (e.g., *n*-hexanol), and a neutral surfactant (hexadecylamine). However, other neutral and cationic surfactants also could be used, such as *n*-decylamine and hexadecyltrimethylammoniun [34]. The surfactant/alumina molar ratio in the synthesis mixture varies in the range 0.072–0.288, whereas the silicon alkoxide/alumina molar ratio in the gel can vary in the range 0.1–1.5.

2.2.2. Synthesis with hexadecylamine

A solution of 34.31 g of phosphoric acid (Riedel de Haën, 85 wt%) in 30 g of water was added on 20.34 g of alumina (Pural SB, Condea, 74.6 wt%) placed in a 500-cm^3 polypropylene bottle provided with a cap, which has a central hole large enough to accommodate the axis of a Teflon paddle stirrer. The bottle was placed in a water bath kept at 293 K, and the resulting mixture was stirred for 2 h at 350 rpm. Then 15.21 g of dipropylamine (Aldrich) are added under stirring, which was maintained for 2 h. Subsequently, a solution of 68.27 g of hexanol (Aldrich), 5.75 g of hexadecylamine (Aldrich), and 30 g of distilled water was added, followed immediately by 9.30 g of tetraethylortosilicate (MERCK-Schuchardt, $>98\%$) and 26.81 g of distilled water. This mixture was stirred for 2 h (final pH $= 4.3$) and introduced into six 60-cm^3 autoclaves

with Teflon liners heated statically at 468 K for 24 h. Subsequently, the mixture was centrifuged, and the recovered solid was washed with water, ethanol, and water again and then dried at 313 K overnight. In this way, 37.13 g of solid product was obtained, which was designated as SAPO-11 by XRD, with minor amounts of SAPO-41.

In another example, the silicon alcoxide content of the reaction mixture was reduced, and 3.27 g of TEOS was used to obtain a silica/alumina molar ratio of 0.1 in the gel, keeping the remaining reactants and the crystallization conditions unchanged. The solid product was identified as SAPO-11 by XRD, with minor amounts of SAPO-41.

SAPO-11 of higher purity can be obtained by reducing the surfactant concentration in the gel. In this way, a gel with molar composition Al_2O_3:P_2O_5:0.5 TEOS:1.0 DPA:0.072 hexadecylamine:4.4 hexanol:40 H_2O was prepared in the same way and crystallized under the same conditions as in the previous examples. The product can be identified as highly crystalline SAPO-11.

The samples were calcined at 823 K under a continuous flow of N_2 (130 cm^3/min) for 1 h, followed by air (130 cm^3/min) for 1 h. Samples obtained from surfactant-contained gels were designated as SAPO-11S.

2.3. Characterization

Power XRD data of the materials were recorded in a Philips X'Pert MPD diffractometer equipped with a PW3050 gioniometer (Cu$K\alpha$ radiation, graphite monochromator) provided with a variable divergence slit. The morphology and mean crystallite size of the SAPOs were obtained from scanning electron microscopy (SEM) photographs (Philips XL30).

The elemental composition of the samples was analyzed by ASS in a Varian Spectra A-10 Plus apparatus. BET area was determined by N_2 adsorption/desorption with a Micromeritics ASAP 2000 instrument after the samples were pelletized, crushed, and then sieved to obtain the 0.59–0.84 nm fraction.

The total amount of Brønsted and Lewis acid sites, as well as the acid strength distribution, were determined by room temperature adsorption and thermal desorption of pyridine. In those experiments, the samples were first treated in vacuum at 673 K and 0.013 Pa for 3 h. Then 400 Pa of pyridine was admitted at room temperature and allowed to equilibrate with the sample for 1 h. Subsequently, the sample was evacuated at 423 K and 0.013 Pa for 1 h to remove the physically adsorbed pyridine, and the IR spectrum was recorded at room temperature. The same protocol was repeated after evacuation at 523 and 623 K. The extinction coefficients of Emeis were used to quantify the results [36].

Solid-state ^{29}Si NMR spectra were recorded with a Varian VXR S400 WB spectrometer at 79.5 MHz using a 7-mm CP/MAS Varian probe with zirconia rotors. To acquire the spectra, 4.2-μs pulses corresponding to a $\pi/3$ rad pulse length were applied, with a 40-s recycle delay and a rotor spinning rate of 5 KHz. The simulation of the experimental spectra was carried out from individual Gaussian lines using Peak Solve software.

2.4. Catalytic activity

n-Hexadecane (Aldrich, >99%) hydroisomerization was carried out in a stainless steel automated reactor at 4×10^3 kPa, with a H_2/hexadecane ratio of 50 mol/mol and a contact time of 0.279 h. The calcined SAPO-11 samples were impregnated with 0.5 wt% of Pt, starting with a solution of H_2PtCl_6 (Aldrich, >99%), and subsequently treated in air at 773 K for 3 h. Before reaction, the catalyst was reduced in situ in a flow of H_2 (5 cm^3/s) at 723 K for 3 h. Hexadecane conversion and selectivities were measured from chromatographic analysis of effluent streams (Varian 3400) using a capillary column (DH50 cross-linked methylsilicone column, 50 m × 0.32 mm, 1.05-μm film) and a flame ionization detector. Hexadecane conversions are reported as the percentage of *n*-hexadecane fed that disappeared during the reaction. Product selectivities are reported on a carbon basis as the percentage of the converted *n*-hexadecane appearing as each product.

3. Results and discussion

3.1. Synthesis and characterization

Two series of SAPO-11 samples with varying Si content were synthesized using a conventional procedure [35] and using the synthesis method described in Section 2, which involves the presence of surfactant in the synthesis gel in biphasic media. For comparison, SAPO-11 samples in biphasic media but in absence of surfactant were also tried; however, the SAPO-11 structure was not obtained, at least in the same gel composition range used for preparation of the SAPO-11 with surfactant. SAPO-11 in biphasic media could be obtained following the procedure described previously [37]; however, its catalytic activity is very low. Thus, for comparison, here we show two SAPO-11 series prepared by conventional procedures and using surfactants.

Fig. 1 shows the powder XRD patterns of the calcined samples synthesized with and without surfactant. In all samples, the peak positions and intensities are identical to those reported for SAPO-11 [38]. The samples prepared with surfactant show line broadening indicating the existence of small crystallites. This was confirmed by SEM (see Fig. 2); the average crystallite sizes are given in Table 1. BET and microporous surface areas of the samples are also given in Table 1. It can be seen there that the samples synthesized with surfactant have smaller microporous surface areas, possibly due to their smaller crystallite size.

Table 2 gives the total number of Brønsted and Lewis acid sites measured by pyridine adsorption–desorption. The results indicate that the total amount of acid sites in the SAPO-11 samples synthesized using surfactant increases with increasing silicon content, whereas within the same range of composition, the number of acid sites decreases in the SAPO-11 samples synthesized in the absence of surfactant. Moreover, although similar amounts of total acid sites can be achieved by the two synthesis methods (see samples SAPO-11C1 and SAPO-11S3 and S4), the numbers of sites with strong to medium acidity (pyridine

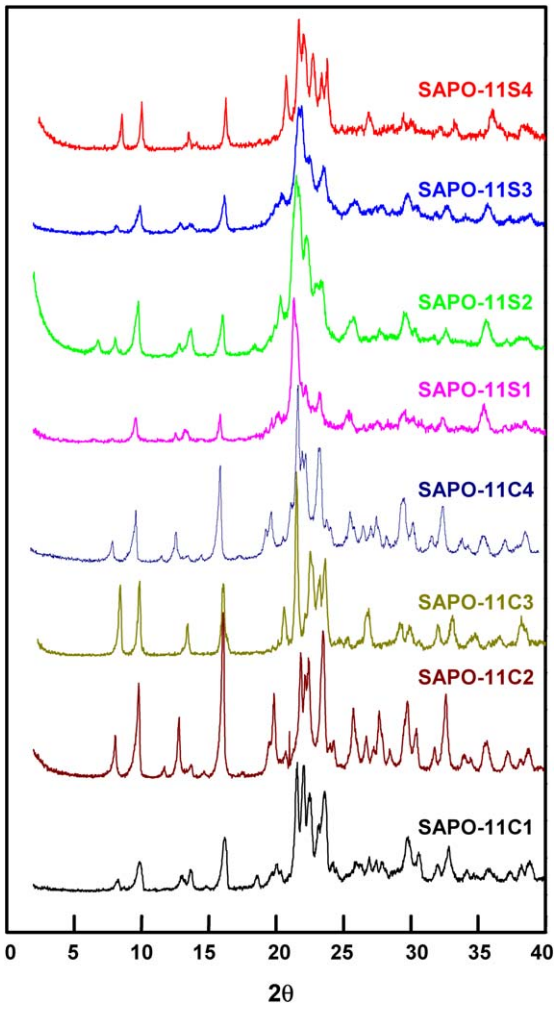

Fig. 1. XDR patterns of calcined SAPO-11 samples synthesized with surfactant (series S1, S2, S3 and S4) and without surfactant (series C1, C2, C3 and C4).

desorption at $T \geqslant 523$ K) are higher for the samples synthesized with surfactant in the entire range of composition studied here. Therefore, the new synthesis route using surfactant gives SAPO-11 samples with similar total amounts of acid sites as obtained through conventional synthesis methods, but a higher proportion of sites with medium to high strength. As shown below, this behavior is in agreement with the changes in the Si chemical environment detected by NMR.

In contrast to aluminosilicate zeolites, the number of bridging hydroxyls cannot be derived directly from the chemical composition of the SAPO materials, because their acidic properties depend on the way in which the silicon atoms are incorporated into the framework. The incorporation of Si atoms into the aluminophosphate frameworks occurs through two different mechanisms [39]. The substitution of a Si atom by a P produces an isolated Si(4Al) environment in which the Al contains P atoms into its fourth coordination shell, giving rise to acid sites of weak strength. The second mechanism involves the substitution of an Al–O–P pair by two silicon atoms combined with substitution of the three P atoms adjacent to the aluminum by three more Si, to avoid the formation of Si–O–P bonding. This second incorporation mechanism leads to the appearance of silica islands with a minimum size of five silicon atoms immersed into the aluminophosphate network. This will produce a ^{29}Si NMR spectrum consisting of signals of Si(4Si), but also of Si (4nSi, nAl) environments generated at the bor-

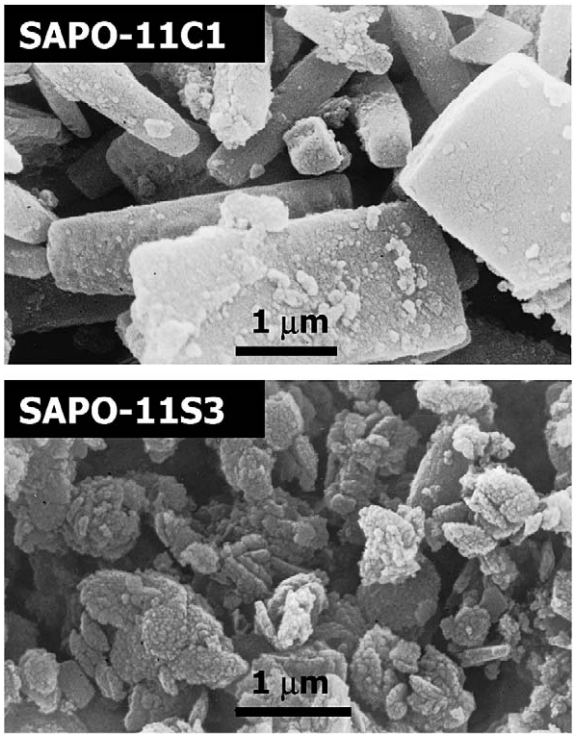

Fig. 2. SEM micrographs of samples SAPO-11C1 (synthesized without surfactant) and SAPO-11S3 (synthesized with surfactant).

Table 1
Textural properties of SAPO-11 samples calcined at 823 K

Catalyst	Si (wt%)	BET area (m^2/g)	Microporous		External surface area (m^2/g)	Crystallite size (μm)
			Surface area (m^2/g)	Volume (cm^3/g)		
SAPO-11C1	1.8	178	146	0.249	32	2 × 1
SAPO-11C2	2.5	177	130	0.233	47	0.12
SAPO-11C3	3	173	128	0.222	45	0.10
SAPO-11C4	6	175	124	0.231	51	0.12
SAPO-11S1	1	179	94	0.219	85	0.07
SAPO-11S2	3.1	174	86	0.218	88	0.08
SAPO-11S3	5.1	176	99	0.217	77	0.09
SAPO-11S4	10.2	177	97	0.215	80	0.08

Table 2
SAPO-11 acidity measurement by adsorption–desorption of pyridine at different temperatures

Catalyst	Si (wt%)	Brønsted (μmol Py/g)			Lewis (μmol Py/g)		
		423 K	523 K	623 K	423 K	523 K	623 K
SAPO-11C1	1.8	18	8	1	6	4	2
SAPO-11C2	2.5	16	9	1	6	4	2
SAPO-11C3	3	13	9	0	4	3	2
SAPO-11C4	6	13	8	1	5	3	1
SAPO-11S1	1	10	7	1	5	3	1
SAPO-11S2	3.1	14	13	2	5	6	3
SAPO-11S3	5.1	19	12	4	10	7	4
SAPO-11S4	10.2	18	13	1	10	8	–

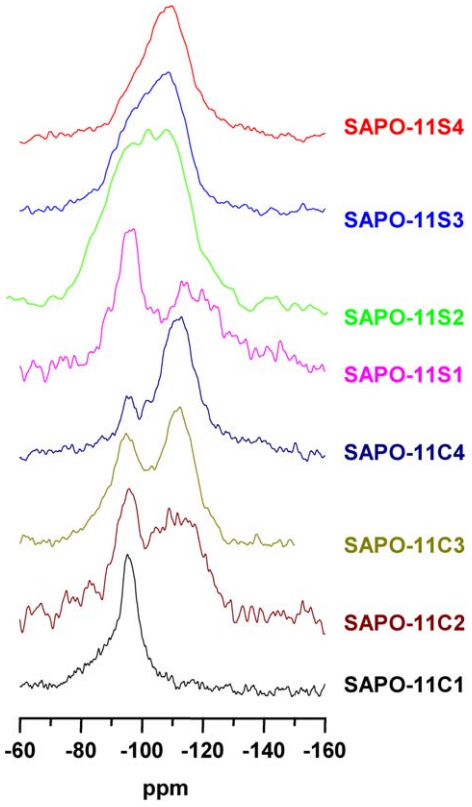

Fig. 3. ^{29}Si MAS-NMR spectra for calcined SAPO-11 samples synthesized using surfactant (series S1, S2, S3 and S4) and without surfactant (series C1, C2, C3 and C4).

der of the SiO_2 patches. The relative intensity of the different signals will be determined by the size of the silica domain. In this case, whereas the silicon atoms belonging to the inner position of the SiO_2 domains do not generate acidity, acid sites similar to those of aluminosilicates will appear at the border of the patches [33]. Moreover, the presence of a small component at lower fields has been attributed to Si(4Al) originating within the silica patches [33].

We used ^{29}Si MAS-NMR spectroscopy to investigate the distribution of silicon in our SAPO samples. Fig. 3 shows the ^{29}Si MAS-NMR spectra of the samples synthesized with and without surfactant after the removal of the organic phase by calcination. Important differences in Si distribution can be observed as a function of the synthesis method. The spectra of the SAPO-11 samples synthesized without surfactant are constituted mainly by an intense peak at ≈ -110 ppm assigned to silicon atoms in Si(4Si) environment and a second component at -94 ppm, probably resulting from the contribution of a peak at ca. -90 ppm of Si(4Al) and other peaks of Si(4-nAl). The spectra of samples prepared with surfactant consists of a very broad and unstructured resonance with higher intensity in the chemical shift range between -80 and -120 ppm, suggesting a higher population of silicon environments of type Si (nAl, 4-nSi) with $0 < n < 4$. The differences become especially evident when we compare the spectra of samples with the same silicon content prepared by the two different procedures, that is, samples SAPO-11S1 and SAPO-11C1, C3 and S2, and C4 and S4. Whereas in samples prepared by the conventional method, the Si(4Si) component is the most prominent, in the latter samples, the maximum appears at an intermediate position.

To illustrate the presence of different silicon environments, we have simulated the experimental spectra of samples synthesized with and without surfactant using individual Gaussian lines (Fig. 4). As Fig. 4 shows, the spectra can be simulated by the contribution of five peaks at ca. -88, -97, -103, -108, and -112 ppm, which can be attributed to Si(4Al), Si(3Al, 1Si), Si(2Al, 2Si), Si(Al, 3Si), and Si(4Si) environments, respectively.

Following the models proposed for silicon incorporation in aluminophosphate framework [33], the differences observed in the ^{29}Si MAS-NMR spectra of the SAPO-11 materials studied here can be interpreted as resulting from different sizes of the siliceous patches. For the same silicon content, the formation of small islands will lead to a higher relative concentration of Si (nAl, 4-nSi), $0 < n < 4$, border environments, whereas in large patches, Si(4Si) sites will be predominant. It is remarkable that the samples synthesized using surfactant, even for higher Si amounts, give a much lower amount of Si(4Si) than the samples obtained without surfactant, supporting the proposition that the introduction of surfactant during synthesis contributes to better Si dispersion, thereby increasing the number of acid sites.

3.2. Catalytic activity

The isomerization reaction of n-hexadecane was carried out with the SAPO-11 catalysts at various temperatures; the conversions obtained over the samples synthesized in the presence and absence of surfactant are shown in Figs. 5a and 5b, respectively. The results indicate that a higher activity was attained with SAPO-11 catalysts synthesized in the presence of surfactant in the whole temperature range. The effect of silicon content on n-hexadecane conversion at 593 K for the two series of samples is depicted in Fig. 6.

The greater activity obtained with SAPO-11 catalysts synthesized with surfactant can be explained by their smaller crystallite size, as well as by the greater activity generated by different silicon distributions. Indeed, comparing the activity of SAPO-11C3 and SAPO-11S2, both with very similar Si content and very close crystallite size, clearly shows that SAPO-11S2 has a much higher activity (10 and 60% of conversion, respectively, at 573 K). A similar conclusion can be drawn by comparing SAPO-11C4 and SAPO-11S3 (4 and 50% of conversion, respectively, at 373 K). These results clearly suggest that the differences in catalytic activity between the two catalysts series cannot be due solely to differences in the crystallite size, and thus external surface area, but should be better related to the different Si distribution and the corresponding acidity in both series of samples. Certainly, it must be taken into account that the specific activity of the sites of medium to strong acid strength for the isodewaxing reaction (i.e., those present at the border of the silicon islands) must be much higher than that of mild, isolated Si(4Al) sites. Indeed, similar behavior has been reported

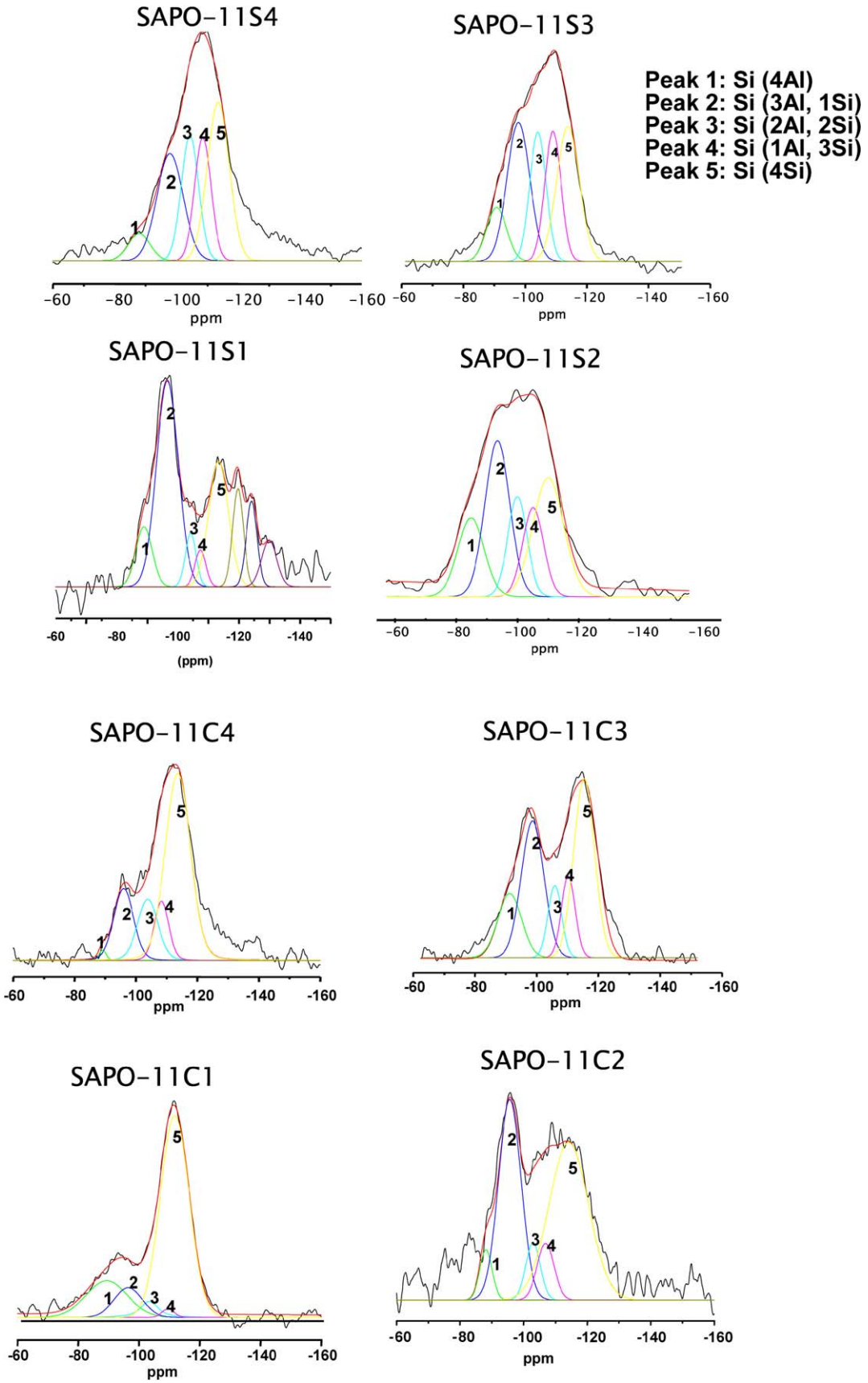

Fig. 4. ^{29}Si MAS-NMR spectra for calcined SAPO-11 samples synthesized using surfactant (series S1, S2, S3 and S4) and without surfactant (series C1, C2, C3 and C4). Experimental (—) and simulated (—) spectra using the peaks constituents [(—) Si(4Al), (—) Si(3Al, 1Si), (—) Si(2Al, 2Si), (—) Si(1Al, 3Si), (—) Si(4Al)]. (For interpretation of the references to colour in this figure legend, the reader is referred to the web version of this article.)

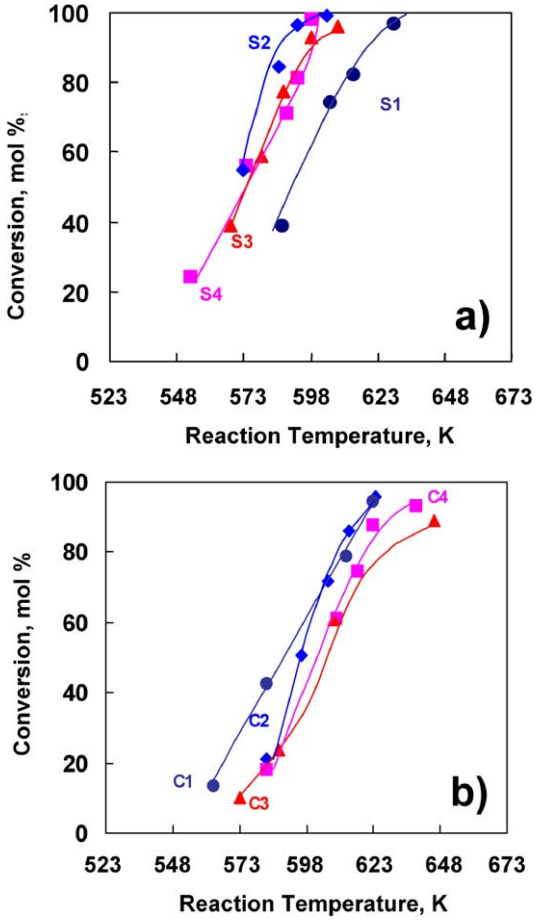

Fig. 5. Conversion of *n*-hexadecane over SAPO-11 versus reaction temperature. (a) Samples synthesized with surfactant: (●) SAPO-11S1, (◆) SAPO-11S2, (▲) SAPO-11S3, (■) SAPO-11S4. (b) Samples synthesized without surfactant: (●) SAPO-11C1, (◆) SAPO-11C2, (▲) SAPO-11C3, (■) SAPO-11C4. Reaction conditions: total pressure of 4×10^3 kPa, H_2/hexadecane ratio of 50 mol/mol and contact time of 0.279 h.

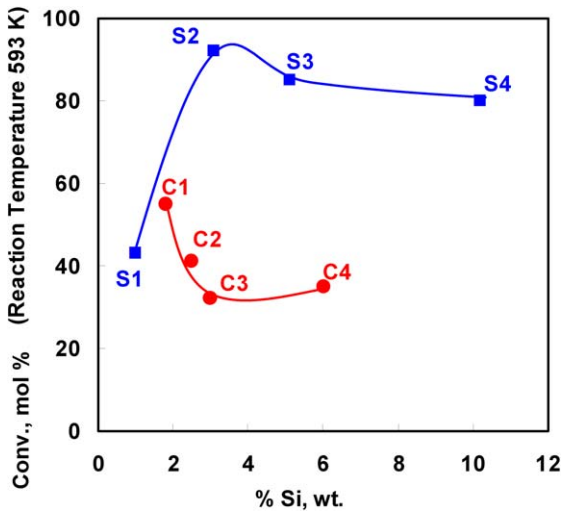

Fig. 6. Variation of conversion of *n*-hexadecane at 593 K over SAPO-11 samples in function of Si content. (■) SAPO-11S samples synthesized with surfactant (S1, S2, S3, and S4). (●) SAPO-11C samples synthesized without surfactant (C1, C2, C3, and C4). Reaction conditions: total pressure of 4×10^3 kPa, H_2/hexadecane ratio of 50 mol/mol and contact time of 0.279 h.

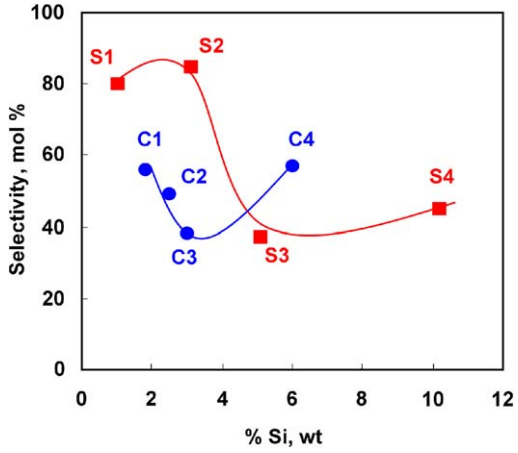

Fig. 7. Variation of selectivity to isomerization during the conversion of *n*-hexadecane over SAPO-11 samples in function of Si content. (■) SAPO-11S samples synthesized with surfactant (S1, S2, S3, and S4). (●) SAPO-11C samples synthesized without surfactant (C1, C2, C3, and C4). Reaction conditions: total pressure of 4×10^3 kPa, H_2/hexadecane ratio of 50 mol/mol, contact time of 0.279 h and 80% of *n*-hexadecane conversion.

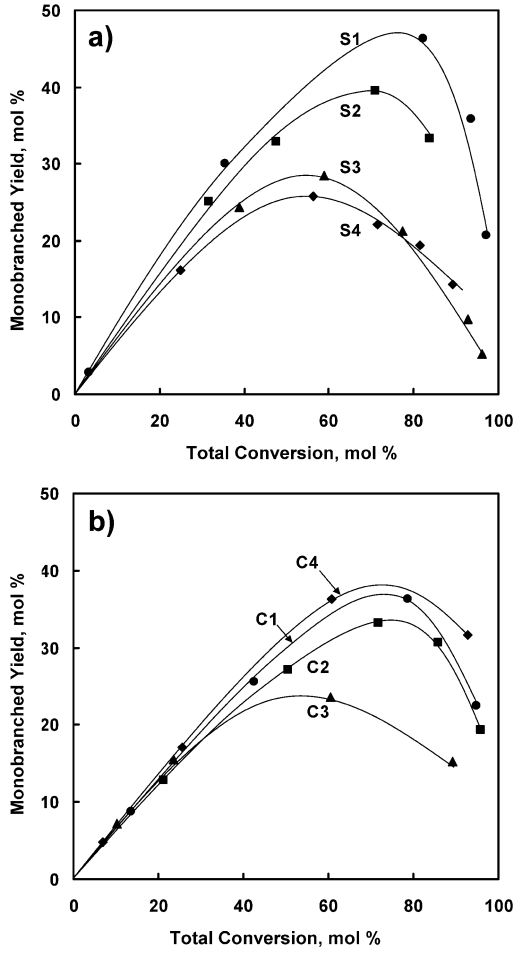

Fig. 8. Total monobranched yields obtained during the hydroisomerization of *n*-hexadecane over SAPO-11 samples versus total conversion. (a) Samples synthesized with surfactant: (●) SAPO-11S1, (■) SAPO-11S2, (▲) SAPO-11S3, (◆) SAPO-11S4. (b) Samples synthesized without surfactant: (●) SAPO-11C1, (■) SAPO-11C2, (▲) SAPO-11C3, (◆) SAPO-11C4. Reaction conditions: total pressure of 4×10^3 kPa, H_2/hexadecane ratio of 50 mol/mol and contact time of 0.279 h.

Table 3
Products distribution yields obtained at 30 and 80% of conversion of *n*-hexadecane over different samples of SAPO-11 synthesized with surfactant (series S1, S2, S3, and S4) and without surfactant (series C1, C2, C3, and C4)[a]

Conversion	Si (wt%)	Monobranched (mol%)		Dibranched (mol%)		Tribranched (mol%)	
		30	80	30	80	30	80
SAPO-11C1	1.8	18.6	36.3	1.2	7.5	0.1	0.2
SAPO-11C2	2.5	16.8	32.2	1.1	7.8	0.2	0.7
SAPO-11C3	3	16.5	18.8	1.3	5.2	0.2	0.2
SAPO-11C4	6	19.8	36.5	1.2	4.6	0.3	0.8
SAPO-11S1	1	26.7	42.1	4.4	21.6	0.7	3.4
SAPO-11S2	3.1	22.8	46.5	3.8	17.3	0.8	3.8
SAPO-11S3	5.1	18.1	20.7	2.4	5.1	1.1	2.5
SAPO-11S4	10.2	18.6	20.7	3.1	12.8	1.9	3.6

[a] Reaction conditions: total pressure of 4×10^3 kPa, H_2/hexadecane ratio of 50 mol/mol and contact time of 0.279 h.

elsewhere for the isomerization of *m*-xylene over SAPO-5 and VPI-5 catalysts synthesized from a two-liquid phase system in presence of surfactants [40–42]. This conclusion will support the idea that isodewaxing occurs not only at the pore mouth (i.e., close to the external surface), but also within the channels of the molecular sieves [31,32].

It can be seen there that the activity goes through a maximum in both series for Si content between 2 and 4 wt%. However, it is also clear that the series synthesized with surfactant gives much higher activity than the synthesized without surfactant, regardless of the Si content.

From the standpoint of selectivity to isomerization (i.e., isomerization with respect to isomerization plus cracking [Fig. 7]), this goes through a maximum in the surfactant series for a Si content between 2 and 4%, which is within the range at which we observed a maximum in activity. All of the conventionally prepared samples give hydroisomerization selectivities below the maximum observed with SAPO-11S2. The detailed analysis of the product distributions summarized in Fig. 8 and Table 3 show that all SAPO-11 samples produce a greater number of monobranched isomers, as is expected for catalysts with this topology [43]. The differences are found when the amounts of dibranched and tribranched isomers are considered, which are greater over the SAPO-11 samples prepared using surfactant (Table 3). Considering the different hypotheses regarding the mechanism of isomerization of long-chain paraffins with this structure [28–31], formation of the multibranched (dibranched and tribranched) isomers can be expected to occur at the catalyst surface. In this case, the higher external surface of the SAPO-11 synthesized using surfactant could justify the greater amounts of dibranched and tribranched isomers obtained. In any case, it is appears that the SAPO-11 materials synthesized in the presence of surfactant allow the preparation of very active and selective catalysts for isodewaxing.

4. Conclusion

Different samples of SAPO-11 have been obtained by adding a surfactant to a two-liquid phase synthesis gel. Samples obtained with this methodology show a different Si distribution than that obtained by conventional synthesis, as has been shown by ^{29}Si MAS-NMR. The Si distribution implies that SAPO-11 samples synthesized using surfactant have a larger number of Brønsted acid sites of medium and strong strength compared with SAPO-11 synthesized in the absence of surfactant.

These new materials with SAPO-11 structure show greater catalytic activity and better product selectivity for isomerization of *n*-hexadecane. The good results that we have obtained make these materials potentially useful catalysts for the production of good-quality lubricant oil.

Acknowledgment

This work was supported by a 1997–1998 research grant from EXXON-Mobil.

References

[1] R.J. Tylor, A.J. McCormack, Ind. Eng. Chem. Res. 31 (1992) 1731.
[2] M.P. Ramage, K.R. Graciani, J.R. Katzer, in: Japan Petroleum Institute Symposium, Tokyo, Japan, 1986.
[3] R.J. Tylor, A.J. McCormack, V.P. Nero, Div. Petrol. Chem. Am. Chem. Soc. 37 (1992) 1337.
[4] S.J. Miller, US Patent 4 859 311 (1989), to Chevron.
[5] S.J. Miller, US Patent 4 859 312 (1989), to Chevron.
[6] A. Corma, J. Catal. 216 (2003) 298.
[7] K.G. Strohmaier, D.E.W. Vaughan, J. Am. Chem. Soc. 125 (2003) 16035.
[8] A. Burton, S. Elomari, C. Chen, R.C. Medrud, I.Y. Chan, L.M. Bull, C. Kibby, T.V. Harris, S.I. Zones, E.S. Vittoratos, Chem. Eur. J. 9 (2003) 5737.
[9] P. Wagner, Y. Nakagawa, G.S. Lee, M.E. Davis, S. Elomari, R.C. Medrud, S.I. Zones, J. Am. Chem. Soc. 122 (2000) 263.
[10] A. Corma, M.J. Diaz-Cabañas, J. Martinez-Triguero, F. Rey, J. Rius, Nature 418 (2002) 514.
[11] A. Corma, F. Rey, J. Rius, M.J. Sabater, S. Valencia, Nature 431 (2004) 287.
[12] A. Corma, M.J. Diaz-Cabañas, F. Rey, S. Nicolopoulus, K. Boulahya, Khalid. Chem. Commun. 12 (2004) 1356.
[13] J.W. Thybaut, N.C.S. Laxmi, J.F. Denayer, G.V. Baron, P.A. Jacobs, J.A. Martens, G.B. Marin, Ind. Eng. Chem. Res. 44 (2005) 5159.
[14] N.C.S. Laxmi, J.W. Thybaut, G.B. Marin, J.F. Denayer, G.V. Baron, J.A. Martens, P.A. Jacobs, Chem. Eng. Sci. 59 (2004) 4765.
[15] J. Weitkamp, P.A. Jacobs, J.A. Martens, Appl. Catal. 8 (1983) 123.
[16] Th.L.M. Maesen, M. Schenk, T.J.H. Vlugt, B. Smit, J. Catal. 203 (2001) 281.
[17] A. Chica, A. Corma, J. Catal. 187 (1999) 167.
[18] Th.L.M. Maesen, S. Calero, M. Schenk, B. Smit, J. Catal. 221 (2004) 241.
[19] J.A. Martens, P.A. Jacobs, J. Weitkamp, Appl. Catal. 20 (1986) 239.
[20] H. Deldari, Appl. Catal. A 293 (2005) 1.
[21] J. Meusinger, H. Vinek, J.A. Lercher, J. Mol. Catal. 87 (1994) 263.
[22] S.J. Miller, Microporous Mater. 2 (1994) 39.
[23] F.G. Dwyer, E.W. Valyocsik, US Patent 5 336 478 (1994), to Mobil Oil Corp.;
D.J. Klocke, J.C. Vartuli, G.W. Kirker, EP Patent 220893 A2 (1987), to Mobil Oil Corp.
[24] M.C. Claude, G. Vanbutsele, J.A. Martens, J. Catal. 203 (2001) 213.
[25] W.J. Ball, S.A.I. Barri, D. Young, EP Patent 104800 A1 (1984), to British Petroleum.
[26] J.A. Martens, R. Parton, L. Uytterhoeven, P.A. Jacobs, G.F. Froment, Appl. Catal. A Gen. 76 (1991) 95.
[27] P. Meriaudeau, Vu A. Tuan, F. Le Febvre, Vu T. Nghiem, C. Naccache, Microporous Mesoporous Mater. 22 (1998) 435.
[28] J.A. Martens, W. Souverijns, W. Verrelst, R. Parton, G.F. Froment, P.A. Jacobs, Angew. Chem. Int. Ed. Engl. 34 (1995) 2528.

[29] W. Souverijns, J.A. Martens, G.F. Forment, P.A. Jacobs, J. Catal. 174 (1998) 177.
[30] P. Meriaudeau, Vu A. Tuan, F. Le Febvre, Vu T. Nghiem, C. Naccache, Microporous Mesoporous Mater. 26 (1998) 61.
[31] G. Sastre, A. Chica, A. Corma, J. Catal. 195 (2000) 227.
[32] M. Chenk, S. Calero, T.M.L. Maesen, T.J.H. Vlugt, L.L. van Bethem, M.G. Verbeek, B. Schnell, B. Smit, J. Catal. 214 (2003) 88.
[33] J.A. Martens, P.J. Grobet, P.A. Jacobs, J. Catal. 126 (1990) 299.
[34] J. Rodriguez-Agundez, J. Perez-Pariente, A. Chica, A. Corma, I.A. Cody, W.J. Murphy, S.J. Linek, W.O. Patent WO 99/61558 (1999), to EXXON-Mobil.
[35] B.M. Lok, C.A. Messina, R.L. Paton, R.T. Gajek, T.R. Cannan, E.M. Flaningen, U.S. Patent 4,440,871, to Union Carbide Corp.
[36] C.A. Emeis, J. Catal. 141 (1993) 347.
[37] J.A. Martens, B. Verlinden, M. Mertens, P.J. Grobet, P.A. Jacobs, in: M.L. Ocelli, H.E. Robson (Eds.), Zeolite Synthesis, in: ACS Symposium Series, vol. 398, Am. Chem. Soc., Washington, DC, 1989, chap. 22.
[38] C. Halik, S.N. Chaudry, J.A. Lercher, J. Chem. Soc. Faraday Trans. 1 85 (1989) 3879.
[39] B.M. Lock, C.D. Messina, R.L. Patton, R.T. Gajek, T.R. Cannan, E.M. Flanigen, J. Am. Chem. Soc. 106 (1984) 6092.
[40] M. Montoya Urbina, D. Cardoso, J. Pérez-Pariente, E. Sastre, T. Blasco, V. Fornés, J. Catal. 173 (1998) 501.
[41] M.J. Franco, A. Mifsud, J. Pérez-Pariente, Zeolites 15 (1995) 117.
[42] S. del Val, T. Blasco, E. Sastre, J. Pérez-Pariente, J. Chem. Soc. Chem. Commun. 735 (1995).
[43] A. Corma, A. Chica, J.M. Guil, F.J. Llopis, G. Mabilon, J.A. Perdigón-Melón, S. Valencia, J. Catal. 189 (2000) 382.